12-2007

EVALUATION OF A COMPUTER VISION TRAFFIC SURVEILLANCE SYSTEM

Robert Graham
Clemson University, babyboy770@gmail.com

EVALUATION OF A COMPUTER VISION TRAFFIC SURVEILLANCE SYSTEM

A Thesis
Presented to
the Graduate School of
Clemson University

In Partial Fulfillment
of the Requirements for the Degree
Master of Science
Civil Engineering

---

by
Robert Lewis Graham, Jr.
December 2007

Accepted by:
Wayne Sarasua, Committee Chair
Ronnie Chowdhury
Jennifer Ogle

ABSTRACT

This thesis presents an evaluation of the accuracy of a novel computer vision traffic sensor - developed by the Clemson University Electrical and Civil Engineering Departments - capable of collecting a variety of traffic parameters. More specific, the thesis examines how the camera height and distance from the travel way affects the accuracy. The details of the quantitative and qualitative evaluations used to validate the system are provided. The parameters chosen to evaluate were volume, vehicle classification, and speed. Experimental results of cameras mounted at heights of 20 and 30 feet and a lateral distance of 10 and 20 feet show accuracy as high as 98 percent for volume and 99 percent for vehicle classification. Results also showed discrepancies in speeds as low as 0.031 miles per hour. Some problems which affected the accuracy were shadows, occlusions, and double counting caused by spillover.

DEDICATION

This paper is dedicated to my parents, Robert & Carolyn Graham, who always supported my dreams; my grandparents, my sister, Felicia, my brother-in-law, Sam and my best friend, Jim Suss, who constantly shared words of encouragement and never let me give up. Lastly, I dedicate this paper to GOD and my Lord and Savior Jesus Christ, who strengths me. Thank you.

ACKNOWLEDGMENTS

The author wishes to acknowledge the many individuals who participated in some aspect of this project. Thanks go to Dr. Wayne Sarasua, Dr. Jennifer Ogle, Dr. Ronnie Chowdhury, Amol Ranade and Neeraj Kanher. Special thanks Neeraj Kanher for processing all the videos.

TABLE OF CONTENTS

Table of Contents (Continued)

LIST OF TABLES

LIST OF FIGURES

CHAPTER ONE

INTRODUCTION

Previous research has found that, although many vehicle detection systems that use computer or machine vision have a high level of accuracy collecting volume and speed data, the majority of these systems must be placed at heights of 35 feet or higher and be located directly over the travel way and/or in close proximity. This is not ideal due to the higher installation and maintenance costs, as well as safety issues associated with placing poles near the travel way. In the past, there has been limited testing of video detection systems. Systems are being approved and used in the field without being thoroughly tested (Grenard, Bullock, Tarko, 2001).

There has been much research done in the area of vehicle detection since the early 1970s. There are currently a few systems available on the market that can calculate traffic volumes and vehicle speeds. Some of the more well-known systems are Autoscope (Econolite Corporation, 2007) and PEEK VideoTrak (PEEK Traffic Corporation, 2007).

Both Autoscope and VideoTrak use virtual detection in calculating volumes and speeds. With the Autoscope system, lines are drawn on the image and are used as sensors. A sensor is placed for each lane in the video sequence (See Figure 1.1).

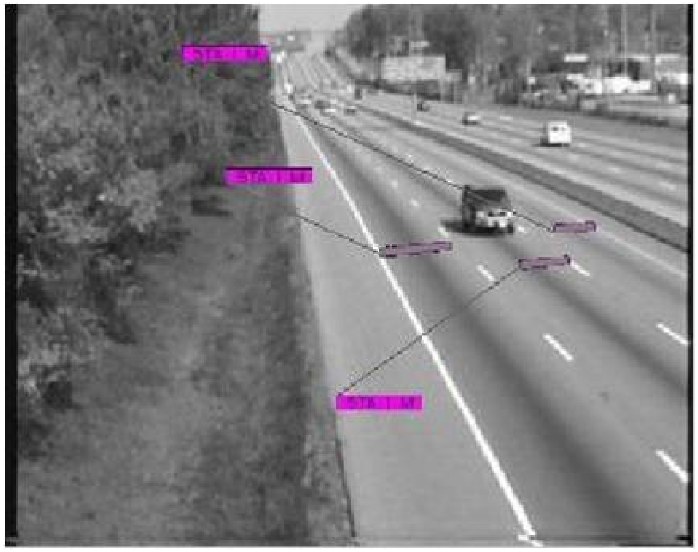

Figure 1.1: Example of virtual roadway sensors.

Video based systems that use virtual detection are prone to errors due to spillover and vehicle occlusions (Michalopoulos, 1991; Oh and Leonard, 2003). Figure 1.2 illustrates an example of spillover as a truck moves across Autoscope virtual detectors that were placed on the lanes. The truck activates all three detectors. The camera used in Figure 1.2 is mounted at 26 feet above the road.

Figure 1.2: Example of spillover.

The VideoTrak system is primarily used for traffic control and surveillance at intersections and on highways. The cameras for this system are typically mounted on poles or on a traffic signal mast arm. VideoTrak's detection algorithm operates along the same lines as the Autoscope system except that the system uses multiple detection zones (See Figure 1.3).

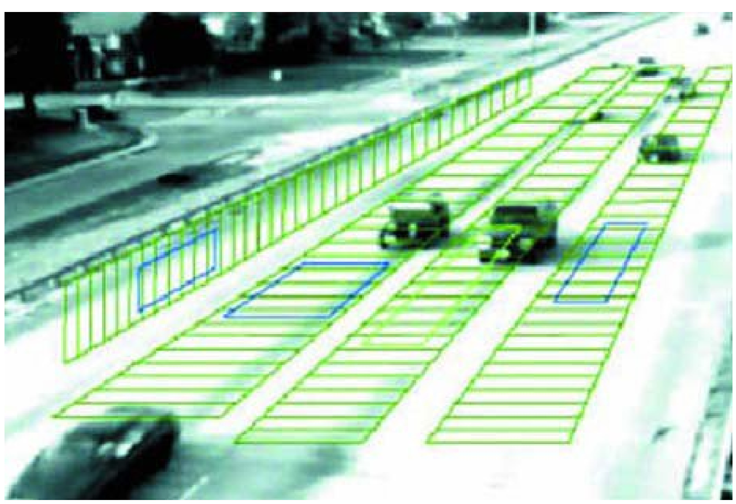

Figure 1-3: Normal detection zone set-up for VideoTrak.

If a vehicle crosses from one detection zone to the other, the vehicle may be counted in both zones. Again, this is another source of false positive detection. The effectiveness of the system decreases as the outside temperature rises above 74°C. In addition to temperature, humidity of higher than 95% will cause the camera lens to condensate (PEEK Traffic Corporation, 2007). One can see how this can pose problems for camera based sensor systems in regions where there is high humidity.

Other problems with machine vision systems identified in the literature include decreased performance in adverse weather conditions and an inability to accurately collect traffic parameters at night in the absence of artificial light (Michalopoulos, 1991; Oh and Leonard, 2003).

Researchers in Clemson's Departments of Electrical Engineering and Civil Engineering have developed a novel computer vision traffic sensor capable of collecting a variety of traffic parameters. The Clemson system differs from commercial based systems. Whenever a vehicle enters the detection zone, a label is placed on that vehicle and remains on the vehicle until it exits the detection zone. This prevents a vehicle from being counted multiple times. A vehicle is tagged as soon as the vehicle comes into view; thus, the effects of occlusions are minimized−even when cameras are placed at lower heights.

An earlier version of the Clemson system tracked only a portion of a vehicle that remains stable throughout the sequence. These were identified as "vehicle base-fronts" or VBFs. The benefit of tracking VBFs is that there is little depth ambiguity as a vehicle moves through the sequence. Computations are simplified because it is not necessary to accurately determine the height of vehicles. The drawback of VBFs is that this method only works well in clear and sunny weather conditions or if the vehicles in the video sequences had headlights on. The algorithm had to be adjusted in order to be able to track vehicles regardless of weather conditions and the amount of ample lighting. This way the system may be operational year-round in any type of weather condition and at any time of day. The current system uses an algorithm which recognizes vehicle features and patterns.

In this thesis, the Clemson system is evaluated both quantitatively and qualitatively. The research objectives focus on determining how camera height and camera distance from the travel lanes affects the level of accuracy of this next generation computer machine vision processor in detecting traffic volumes, vehicle speeds, and vehicle classifications. The effects of the camera angle on accuracy were also studied. The objectives of this thesis are:

- Assess the effects of the camera height and distance from the roadway quantitatively using the following measures of effectiveness:
    - Difference in individual vehicle speeds
    - Difference in mean speeds
    - Difference in 85^{th} percentile speeds
    - Difference in variances
    - Number of false negative and positive detections
    - Percentage of vehicle classified correctly

- Assess the effect of the camera height and distance from the roadway qualitatively including determining the cause of false detections.

This thesis is organized into 5 chapters. The review of literature is discussed in Chapter 2. Chapter 3 outlines the methodology used for this research and provides specific details on how the objectives will be achieved. Chapter 4 discusses the results of the analysis and Chapter 5 provides conclusions and recommendations.

CHAPTER TWO

LITERATURE REVIEW

Vehicle detection and tracking is becoming more of a necessity in traffic engineering. It is a useful tool for volume and speed data collection. Research in this area began around the world in the mid-1970s. Some of the countries leading this research were Japan, France, Australia, England, Belgium, and the United States (Michalopoulos, 1991). One of the first applications of using video detection, in the United States, was employed to detect left-turning vehicles. An optical image device system, including a Color-Capture Device (CCD) video camera, was used. There was only 80 percent accuracy for detecting the left-turning vehicles whose signal lights were on (Yean-Jye, Hsu, and Tan, 1988). Given that this system was the first of its kind, these were fair results.

With traffic congestion problems continuing to grow in urban areas, the need for more advanced intelligent transportation systems became obvious. Development of the first wide-area multi-spot video imaging detection system, in the United States, was developed at the University of Minnesota in 1984; they named the system Autoscope. There were a few issues with previous detection systems that the Autoscope team tried to eliminate with their system. One of the issues pertained to false vehicle detection due to shadows, changes in light and reflections. The new system partially fixed this problem by using vehicle signature detection. Another issue with the older systems dealt with a lack of accuracy operation in conditions with congestion or stopped vehicles. The research team included a background refresh algorithm in order for vehicles to remain stopped for longer periods of time without blending into the background, which would give inaccurate results (Michalopoulos, 1991).

In the wake of new approaches to real-time moving vehicle detection, there were more doors being opened for vehicle detection research. The development of Autoscope led to other methods of detecting and tracking moving vehicles. Vehicle detection systems were being improved to be able to operate in various weather conditions, including sunny, partly cloudy and cloudy. Another approach that came about was using velocity to delineate between moving vehicles and stopped vehicles or objects in the road (Charkari and Mori, 1993).

All research done prior to the early 1990s centered around vehicle detection on urban arterials. A new approach was being proposed for a video-based freeway traffic monitoring system. Transportation engineers were starting to use vehicle detection techniques to monitor freeways and detect possible congestion along the road. They were able to do this by using real-time estimated speeds of the vehicles traveling in different lanes of the freeway (Gloyer, 1995). With more innovations in video vehicle detections and tracking, the costs of these systems were beginning to increase. This need for traffic detection devices that had lower installation, operation, and maintenance costs led to the development of machine vision wide-area detection systems (WADS). Autoscope's WADS is an example of the system that led the pack. Although volume and time occupancy were the only parameters being detected, results indicated that the Autoscope system would be the most cost effective option at the time for wide-area video detection (Michalopoulos, Anderson, and Jacobson, 1996).

Up until this point, detection and tracking systems centered on a single vehicle. Researchers began looking at how to develop a real-time vision system that could recognize and track multiple vehicles on highways and local roads. This required an algorithm that could distinguish moving vehicles within the study area of the frame based on tracking motion parameters that are distinctive for vehicles, such as the recognition of headlights (Betke, Haritaoglu, and Davis, 1997). This research led to the concept of using motion information distinct to various vehicle classes to detect and track vehicles (Rajagopalan and Chellappa, 2000). Another development that continued from multi-vehicle detection research dealt with a real-time vehicle detection system which could analyze color videos. The system used a combination of color, edge, and motion information to recognize and track the road boundaries, lane markings and other vehicles on the road. Cars were recognized by matching templates that were cropped from the input data and by detecting highway scene features and evaluating how they relate to each other. This detection system was one of the first trials for video recording in various weather conditions including difficult visibility situations (Betke, Haritaoglu, and Davis, 2000).

In the early part of the 21st century, other companies began to develop other vehicle detection and tracking systems-one of which was the PEEK VideoTrak 900. This system uses virtual detection zones with limited tracking capabilities. A research team installed 12 PEEK VideoTrak 900s in Atlanta on Interstate Highway I-75. The cameras were mounted at a height of 50 feet about the roadway. They tested the detection of vehicle speed and volume count accuracy of the system. The results of the tests showed that the system provided stable speeds, approximately 10 percent deviation, but gave inaccurate volume counts. There was as much as 20 percent difference in volume counts between various trials. These were the daytime results, but the accuracy of the system decreased as the amount of sunlight diminished (Oh and Leonard, 2003).

Prior to 2005, research for video vehicle detection focused on intersections, urban streets, and highways. Transit monitoring and traffic interaction were beginning to get attention. The interaction between transit and passenger vehicles may have an enormous impact on the performance of a roadway. Another innovation with this research dealt with eliminating fixed-point detection. In contrast to earlier machine vision technologies used for traffic management, this new approach would use an active vision system, in which you can control the camera parameters, such as orientation, focus and zoom. Researcher in this new approach mounted cameras on buses, in order to allow them to get feedback and analyze real-time traffic conditions (Rabie, Abdulhai, and Shalaby, 2005). This study led to research into the interaction of vehicles with the surrounding environment using traffic videos to interpret real-time driver behavior. The forms of interaction studied consist of interaction with other vehicles, between vehicles and stationary objects, and between pedestrians and vehicles (Kumar, et al., 2005).

Another study being conducted around the same time dealt with using video vehicle detection systems as an alternative to loop detectors at actuated intersections on urban streets. Cameras were posted at various heights on a strain pole. The videos and data collected from the loop detectors were reviewed for discrepancies. In conclusion, researchers found the loop detectors gave better accuracy than the cameras regardless of the height. The cameras produced more false detections and missed detections. Research could be continued to see if the type of camera has any effect on results (Rhodes, 2005). Due to the inaccuracies in detection and tracking using traffic videos at intersections, research teams began looking at the use of filters to delineate between moving vehicles and the surrounding environment (Qiu and Yao, 2006; Sun, Bebis, and Miller, 2005).

In recent years, studies have been conducted to measure the effects of heavy traffic flow conditions on the level of response to traffic incidents and how fast changes in these traffic variables can signal the occurrence of an incident. It's been found that many video-based detector systems do not possess the required algorithm and therefore are not able to sustain a desired level of effectiveness in detecting incidents (Mak and Fan, 2006; Kamijo, et. al, 2005).

Over the years researchers in computer vision have proposed various solutions to the issues surrounding automated tracking. A few of the approaches are based on active contour tracking, feature tracking, 3D-model based tracking, and pattern-based tracking. First there is active contour approach, which is based on tracking active contours, which are also known as "snakes", representing the boundary of an object. Vehicle tracking is achieved with the use of two Kalman filters (Koller et al., 1994; Qiu and Yao, 2006); one for determining the relationship between motion parameters, and the other for determining the shape of the contours (Koller et al., 1994). Filters are used to delineate between moving vehicles and the surrounding environment. The Kalman Filtering process has the capability of combining both position and velocity data to obtain better tracking results (Qiu and Yao, 2006).

The second approach is feature tracking, in which feature points on an object are tracked instead of the entire object. In situations where there is some degree of occlusions, this would be the most useful method. The task of tracking multiple objects then becomes the task of grouping the tracked features based on one or more similarity criteria. A study done at the University of California, in Berkley, proposed a feature-based tracking approach for traffic monitoring applications. With this approach, feature points which are tracked successfully throughout the specified detection zone are considered in the process of grouping. In order to acquire accurate groupings, the features on the vehicles need to be tracked over the entire detection zone which is often not possible due to occlusions (Beymer, 1997). There have been studies done dealing with tracking vehicles, at intersections, in order to deal with the issue of tracking occluded features in the detection area. Research is still being done in this area (Saunier and Sayed, 2006).

The next method used for tracking vehicles utilizes three-dimensional models, which have been studied by several research groups (Dandilis, Koller, and Nagel, 1993; Haag and Nigel, 1999; Ferryman, Maybank, Worral, 1998; Hinz, Reitberger, and Schlosser, 2003). One study tracked a single vehicle through a detection region with partial occlusions. The vehicle was successfully tracked, but these results are not necessarily relevant to congested traffic conditions (Ferryman Maybank, Worral, 1998). Another approach uses aerial views of the scenes which practically eliminates with occlusions, and then, matches the three-dimensional version of different vehicle classifications to edges detected in the image (Hinz, Reitberger, and Schlosser, 2003).

The final method is color/pattern-based tracking. One study conducted associated vehicle detections with one another by the use of colors to depict various driver behavior characteristics and probability of arrival for each type (Barber et al., 1997). In addition to tracking vehicles from a stationary camera, research has been conducted using pattern-recognition methods, in which a camera is placed inside a vehicle looking straight ahead. Vehicle detection is then treated as a pattern classification problem using support vector machines. This is a useful feature because the system can capture information from multiple scales and form a compact representation (Bebis, Miller, Sun, 2002).

Recently, more research is addressing the need for methods and procedures for evaluating video detection systems. Two methods for evaluating video detection versus inductive loop detectors which have been researched are the discrepancy method, which comparing the individual occupancy times of inductive loop detectors and video detectors for the same traffic flow; and the likelihood method, which involves determining the probability that a certain type of discrepancy between the inductive loop detectors and video detectors will occur (Grenard, Bullock, Tarko, 2001). Issues arose with the accuracy of the system at night and whenever a vehicle pulled beyond the stop bar. During the nighttime hours, the detection zone length needed to be doubled in order to improve the accuracy of the system. To account for the vehicles that crosses the stop bar, the detection zone needed to be stretched out a few feet beyond the stop bar in order to reduce the number of lost detections (Grenard, Bullock, Tarko, 2001).

Another study looked at the performance of video detectors, at intersections, based on camera location and lighting conditions. Researchers tested three different operating systems. For all trials, four cameras were set up on each approach of a four-way signalized intersection; the first camera located at 40 feet above the roadway looking straight down the travel way, the second camera located at 40 feet above the roadway and offset by 12 feet, the third camera located under the first camera at a height of 25 feet, and the last camera located directly above the detection zone. Results showed that the first three cameras performed similarly when it came to the time it took to detect vehicle at the intersection during daytime. That detection time increased as daylight decreased. The fourth camera performed the best results for daytime and nighttime trials. This camera position is mounted directly over the detection zone and is therefore less susceptible to early activation from headlight reflection. The results were uniform for all approaches. Results also showed that there was no significant difference in the performance between the three systems (Rhodes, Jennings, Bullock, 2005; Rhodes, Smaglik, Bullock, 2005).

Currently there are not any commercial systems with robust tracking capabilities available. This research presents an evaluation a system based on a novel technique of detecting and tracking of vehicles through pattern recognition.   By managing perspective effects and vehicle occlusions, the system should overcome some of the limitations of commercially available machine vision-based traffic monitoring systems that are used in many intelligent transportation systems applications. One area that has yet to be touched on is the use of computer vision processing being used with tilt/pan cameras. The Clemson system is capable of automatically calilbrating and recalibrating as the camera is tilted and panned. This is not possible with systems based on virtual detection because the detections zones would have to be redefined every time the camera is tilted or rotated.

CHAPTER THREE

METHODOLOGY

Providing some background information on how the Clemson system operates will help the reader understand the development of the methodology. The system originally detected and tracked the front side of a vehicle's base, also referred to as a vehicle base front and eventually moved to recognition of vehicle features. Many times, two or more vehicles will appear as a single blob in the foreground mask as a result of partial occlusions and a non-ideal perspective view of the scene. In these types of circumstances, detecting vehicle base fronts aids in sorting out and tracking individual vehicles. When an image frame lacks sufficient evidence to track a vehicle base front by matching alone, feature points associated with a vehicle base front are used to predict and update its location in consecutive frames. Tracking feature points associated with a vehicle base front improves the accuracy of tracking (Birchfield, et. al, 2006). The concept of vehicle base-fronts is illustrated in Figure 3.1. The only problem with vehicle based fronts is the process only works when the weather is clear and sunny or the vehicles being tracked have their headlights on. This is why using pattern recognition is essential so that the system can perform in various lighting and weather conditions.

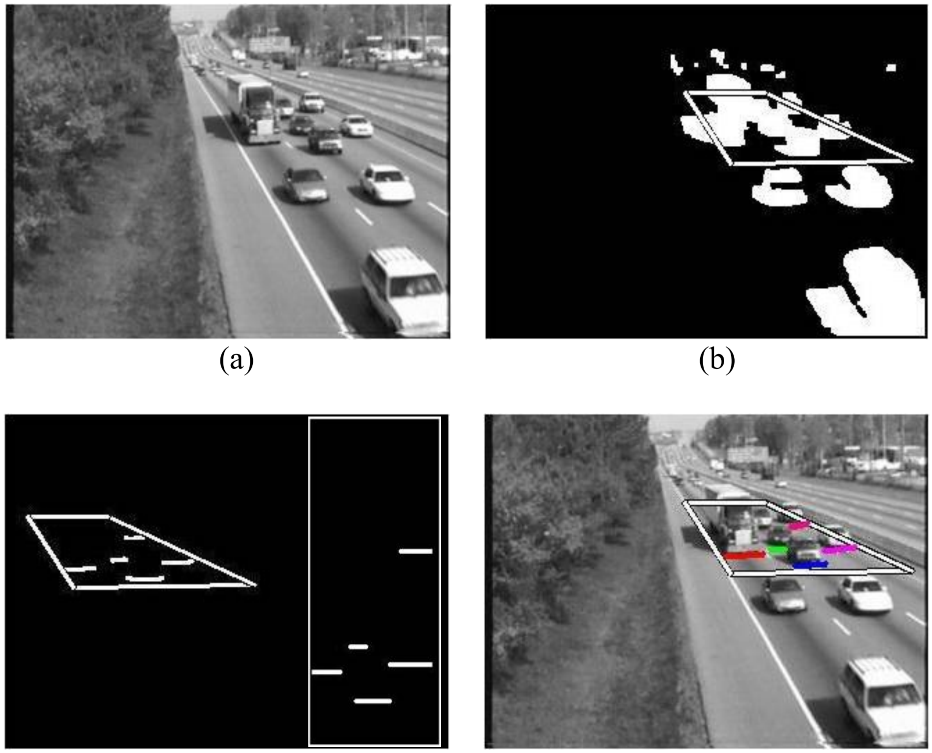

(a) (b) (c) (d)

Figure 3.1: Vehicle base-fronts (a) Input frame. (b) Foreground mask. (c) Detection of base-fronts. (d) Detected vehicles in input frame.

There are some assumptions which must be made in order to use the system: the road surface is flat, the roll angle of the camera is zero, and the primary focal point is the image center. With these assumptions, four parameters are needed to measure the distances on the road within the image: Focal length, tilt angle, pan angle, and height of the camera measured from the road surface (Kanhere, Birchfield, and Sarasua, 2007).

The first step in the process is calibration of the system in order to account for scale changes due to perspective effects and effectively detect vehicle base fronts and features. Simply, the user must first indicate four points along the roadway; and then, specify the width, length, and number of lanes in the detection zone formed by these points, which is illustrated in Figure 3.2 (Birchfield, et. al, 2006).

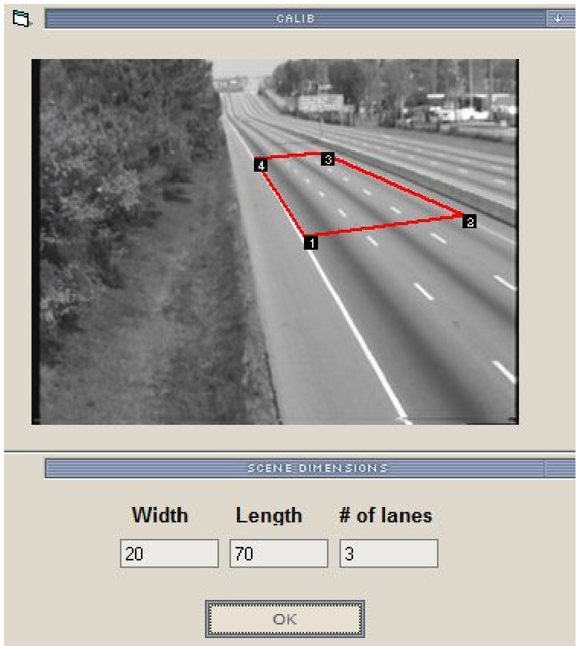

(a)

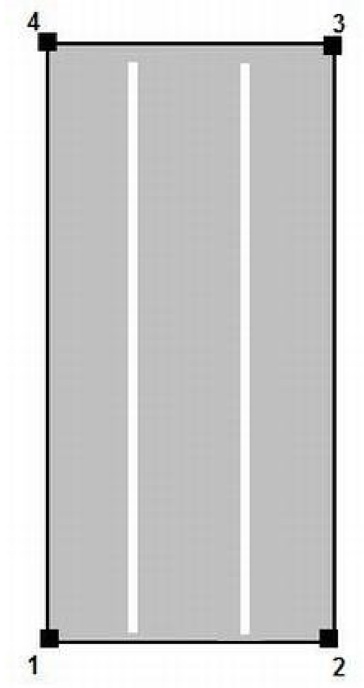

(b)

Figure 3.2: Calibration setup (a) Calibration tool (b) Top-view of detection zone (Birchfield, et. al, 2006)

The next step in the process is background separation. Background subtraction is the technique for pulling out the foreground objects from a scene. The process of background subtraction involves maintaining a background model of the scene. At run time, the estimated background image is subtracted from the input frame in order to produce foreground blobs. A review of different methods for doing background separation modeling can be found in (See Figure 3.3) (Cheung and Kamath, 2004).

Moving shadows are a major problem for successful detection and tracking of vehicles in most tracking algorithms. There are many techniques for detecting moving shadows in both color and grayscale images. A summary of different techniques for detecting moving shadows in grayscale and color images is presented in (Prati, et. al, 2003; P. Rosin and T. Ellis, 1995). Vehicles from the previous image frame are tracked by searching between nearby detections in the current image frame. In case a match is not found, the vehicle is flagged as missing and its location is updated. If a vehicle is missing for several consecutive frames, it is discarded for the lack of sufficient evidence (Kanhere, Birchfield, and Sarasua, 2007).

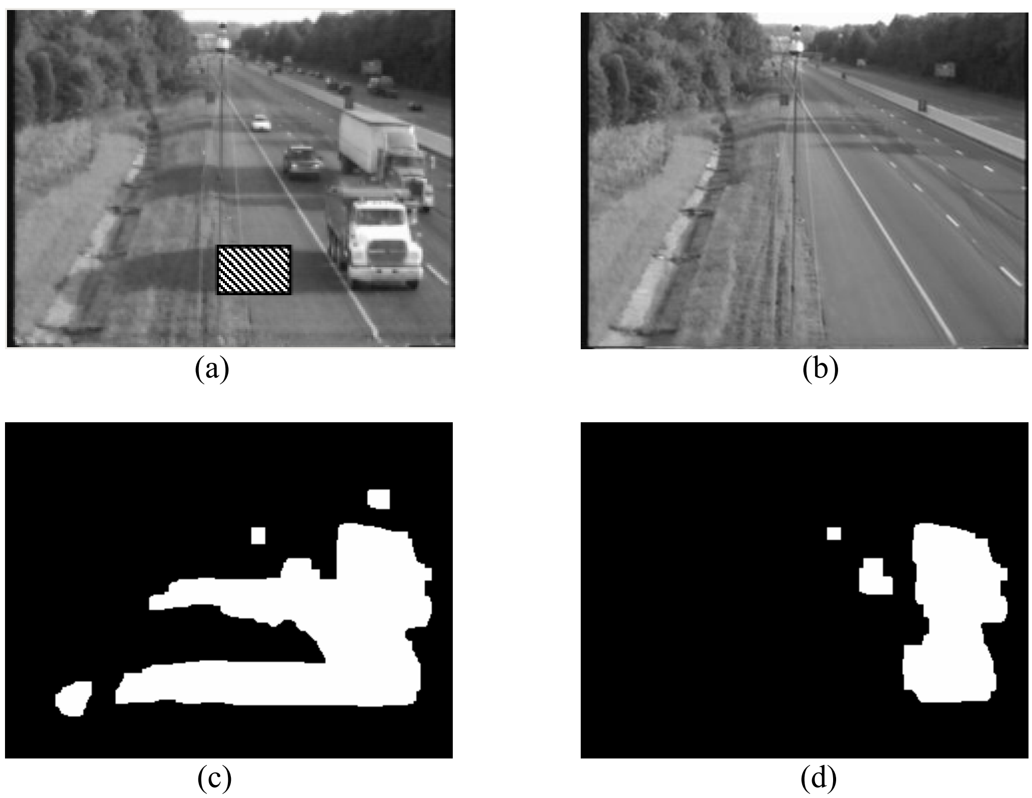

Figure 3.3: Background separation (a) Input frame. Pixels in hatched region are monitored for shadows. (b) Computed background image. (c) Foreground mask without shadow detection. (d) Foreground mask with shadows detected and removed. (Birchfield, et. al, 2006)

One of the most important portions of the process is detection training. This is done by running various video sequences through the program. The system needs to be trained in order to learn vehicle patterns and features. Once this is done, the system can do pattern recognition. The system is capable of pattern recognition after two training sequences; however, the more sequences used for training purposes, the higher the accuracy of the algorithm output.

As mentioned in previous studies (Birchfield, et. al, 2006 and Kanhere, Birchfield, Sarasua, 2007), the evaluation of the new system was based on the comparison of manual versus algorithm counts and speeds as well as on consistency of the algorithm. First, the author wanted to determine how the camera's height and distance from the travel lane affected the accuracy of the algorithm. The distances from the edge of the travel lane used for this study were 10 and 20 feet. For every distance, video sequences were recorded at camera heights of 20 and 30 feet and for an approximate length of 15 minutes. Figure 3.4 illustrates a typical camera setup for recording videos. The camera is located at a height of approximately 30 feet.

Figure 3.4: Typical camera setup for recording videos.

Originally, additional sequences were recorded at heights of 15 and 25 feet. After initial analysis, it was determined that there was not sufficient difference in viewpoints between the heights of 15 and 20 feet, as well as between 20 and 25 feet. Based on engineering judgment, using 20 feet would allow for better comparison. For this study, we recorded and analyzed traffic along Interstate 85 corridor between Clemson, SC and Elberton, GA. The exact locations were milepost 10.5 and milepost 178.

Both locations had similar geometry, i.e. number of lanes, grade, etc, and traffic. It was essential, for safety, to pick locations with a median and significant shoulder width. All video sequences recorded at milepost 10.5 were at a distance of 10 feet from the travel lanes; all video sequences recorded at milepost 178 were at a distance of 20 feet from the travel lanes.

Video sequences were recorded using two analog traffic cameras during evening rush hour, i.e. 3:30 to 7:00 p.m., in various weather conditions, such as cloudy, partly cloudy, and clear/sunny. For the first two recordings, the two cameras were pointed at two different locations in order to evaluate the effect of the tilt and pan angles on detection. With each sequence, the camera viewpoint was centered on a fixed object along the roadway, such as a tree or a roadway marking (See Figure 3.5).

Regardless of the object used as a focal point, it must remain constant for sequences which shared the same distance from the travel lanes. The use of a common focal point allowed for an accurate comparison of angle affects on accuracy and consistency. Figure 3.6 illustrates the locations of the focal points used for this research.

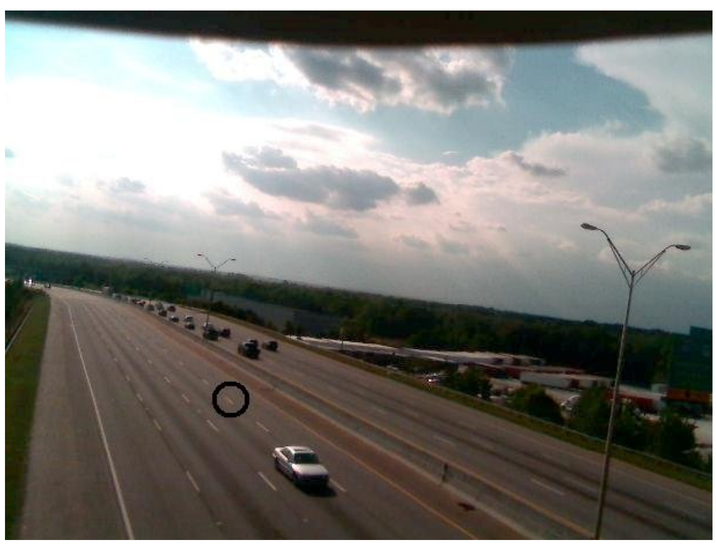

Figure 3.5: Example of roadway marking used as focal point.

Figure 3.6: Focal points used during data collection.

For vehicle speed collection, doing a one-to-one comparison on the recorded speed data and algorithm speeds would provide a more robust statistical comparison. The best way to do this in the field was to place cones at various distances from the camera. These distances had to be adjusted in the field based on their visibility. An example of the cone locations for one of the sequences is illustrated in Figure 3.7. The purpose of the cones on both sides of the road was so that virtual lines could be drawn on the program screen, which is illustrated in Figure 3.8. In some sequences, there was a cone out of the screen, therefore the cone's location had to be estimated.

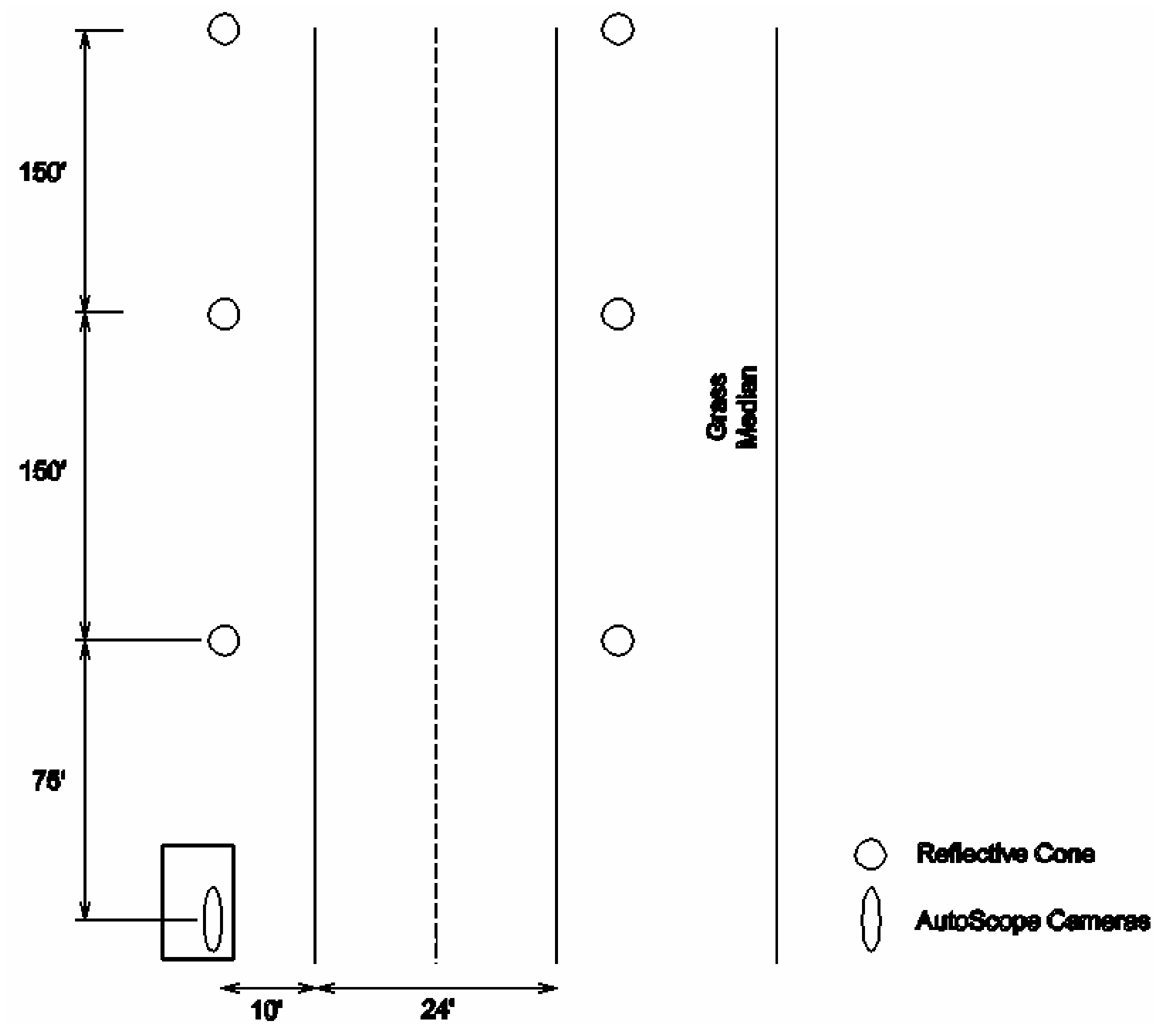

Figure 3.7: Location sketch for data collection.

Figure 3.8: Virtual lines used for estimating speed.

The system computes the speed of a vehicle using the distance traveled, the corresponding number of frames, and the frame rate. To determine the speed of each vehicle manually, the same method could be applied. This would be more accurate than using a stop watch in real time and would provide the most fair assessment of the effect of camera height and distance from the travel way has on the algorithm's ability to calculate accurate speeds.

Originally, video sequences were recorded at a rate of 15 frames per second. This setting was too slow for the algorithm to process the videos. Therefore, the recording speed was increased to 30 frames per second and this setting was used for the remainder of the study.

CHAPTER FOUR

ANALYSIS RESULTS

The first five minutes of each of the video sequences were used for analysis. Traffic operated at a level of service of A or B for every sequence. For volume and vehicle classification comparisons, the video sequences were watched and the volume data and vehicle classification were recorded. These manual values were then compared with those calculated by the algorithm. We define a car as a vehicle with two axles, and a truck as a vehicle with more than two axles. Passenger vehicles towing trailers were not classified as trucks. Only freight vehicles, 18-wheelers, and emergency vehicles of significant length, etc. were classified as such.

Volume Analysis Results

The analysis shows that the volume count accuracy of the system ranges from approximately 94 to 98 percent, while the accuracy of the system to classify the vehicles correctly ranged from 97 to 99 percent. A summary is provided in Table 4.1. Be advised that the accuracy of the vehicle classification is based on the vehicles which were actually detected and counted by the system. Occlusions were an issue for every height and distance, causing missed detections. Double counting was an issue for all but one of the sequences and shadows were an issue for only one of the sequences. Table 4.2 summarizes the total number of false negatives due to occlusions and shadows as well as the number of false positives due to double counting.

Table 4.1: Summary of accuracy of volume and vehicle classification

Video Sequence	Volume Accuracy (%)	Vehicle Classification (%)
D10 H20 (1)	94.29	97.14
D10 H20 (2)	95.28	98.11
D10 H30 (1)	98.08	99.04
D10 H30 (2)	94.39	99.07
D20 H20 (1)	96.52	98.26
D20 H30 (1)	96.58	97.44
NOTE: D = distance from travel way (ft), H = camera height (ft), (#) = focal point		

Table 4.2: Summary of false positives and negatives

	False Positives	False Negatives		Total Number of Vehicles Detected
	Double Count	Shadow	Occlusion	
D10 H20 (1)	8	0	3	107
D10 H20 (2)	9	0	4	110
D10 H30 (1)	1	0	4	103
D10 H30 (2)	3	0	6	104
D20 H20 (1)	4	0	4	115
D20 H30 (1)	0	2	2	113
NOTE: D = distance from travel way (ft), H = camera height (ft), (#) = focal point				

An example of a missed detection due to a partial occlusion is illustrated in Figure 4.1. There was a mix of partial and complete occlusions in each of the sequences. An example of a vehicle in the shadow of another is illustrated in Figure 4.2. The truck traveling in the lane closest to the camera was never detected by the system.

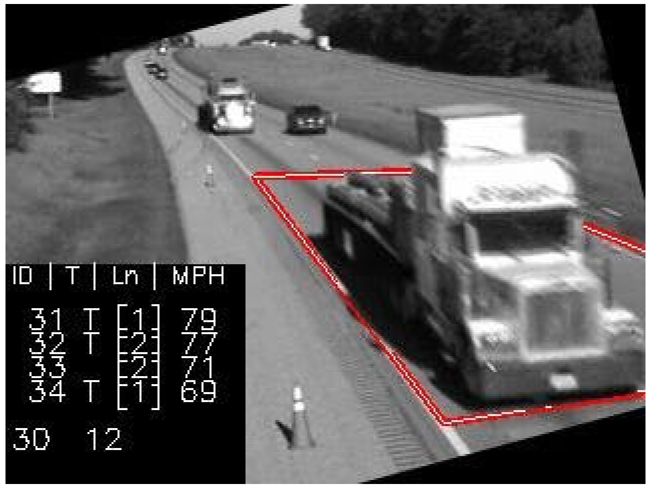

Figure 4.1: Example of a missed detection due to partial occlusion.

Figure 4.2: Example of a missed detection due to shadows.

Since the system uses background separation, vehicles in the shadows of another vehicle would be subtracted along with the shadow itself. It is not possible, though, to conclude whether the height and distance from the travel way plays a role since the sun was not in the exact same location for each sequence.

There were issues with some vehicles being double counted. This could be based on coding errors due to the fact that the system located a large number of feature points and just assumed that a single vehicle was multiple vehicles. Passenger vehicles towing or another vehicle were be seen as two separate entities by the system if there was a large headway between the vehicle and what was being towed.

The system classified vehicles by measuring the total length of the vehicle when it passed through the detection zone. At this stage in the study, the system can only classify vehicle as passenger cars and trucks. Therefore, vehicles towing trailers or another vehicle, without a significant gap between the two, were classified as trucks since their length is similar of that of a freight truck.

Speed Analysis Results

For speed comparisons, the manual and algorithm speeds were calculated using the distance traveled, the corresponding frames, and the frame rate. This would allow for an accurate comparison between the results. The formula used to calculate speed is

$$\text{Speed (mph)} = 0.6818*D*[30\text{fps} / (\text{End frame} - \text{Start frame})]$$

where D = distance traveled

Start frame = frame vehicle enters detection zone

End frame = frame vehicle exits detection zone

Analysis shows that camera height has no significant effect on the accuracy of the speeds determined by the program. However, the camera distance from the travel way drastically effects to calculated speed. This shows that there is a threshold for the pan angles, but the threshold seems to only have a negative effect on the accuracy of vehicles speeds, and not the volumes.

T-test for comparison of Means

According to the two-tailed t-test of the mean outlined in (Ott and Longnecker, 2000), there is a significant difference between the manually calculated speeds and the speeds determined by the system for the sequences recorded 10 feet from the travel way and a height of 30 feet, based on 95 percent confidents. Table 4.3 summarizes the results comparison of means.

Table 4.3: Summary of results for comparison of means

Sequence	Difference in Means	Significant Difference?
D10H20(1)	1.280	No
D10H20(2)	0.768	No
D10H30(1)	16.524	Yes
D10H30(2)	16.027	Yes
D20H20(1)	0.547	No
D20H30(1)	0.031	No

NOTE: D = distance from travel way (ft), H = camera height (ft), (#) = focal point

F-test for comparison of Variances

Using the F-test for comparison of variances outlined in (Ott and Longnecker, 2000), the only sequence with a significant different between the manually calculated speed variance and the algorithm variance was the second sequence recorded at a distance 10 feet from the travel way and 30 feet above the roadway. It seems that the tilt angle affects the overall results as the camera height gets higher. Tables detailing the hypotheses used may be found in Appendix A. Table 4.4 summarizes the results for the comparison of variances.

Table 4.4: Summary of results for comparison of variances

Sequence	Difference in Variances	Significant Difference?
D10H20(1)	6.270	No
D10H20(2)	16.268	No
D10H30(1)	14.238	No
D10H30(2)	26.457	Yes
D20H20(1)	11.885	No
D20H30(1)	0.451	No

NOTE: D = distance from travel way (ft), H = camera height (ft), (#) = focal point

Chi-squared Tests

Based on the chi-squared test for normalcy outlined in (Roess, et. al., 2001), the algorithm speed data appears to be normally distributed for every sequence. Details for each of the chi-squared test are located in Appendix B. The manually calculated speeds were also checked for normalcy. The manually calculated speeds were normally distributed for every sequence except for the sequence recorded at a height of 30 feet, distance of 10 feet and centered on focal point 1. Details for each of the chi-squared test are located in Appendix C. Table 4.5 summarizes the results from the normalcy chi-squared tests for the algorithm speeds and manual speeds.

Table 4.5: Summary of Chi-squared Normalcy Test

	Normally Distributed?	
Sequence	Algorithm	Manual
D10H20(1)	Yes	Yes
D10H20(2)	Yes	Yes
D10H30(1)	Yes	No
D10H30(2)	Yes	Yes
D20H20(1)	Yes	Yes
D20H30(1)	Yes	Yes
NOTE: D = distance from travel way (ft), H = camera height (ft), (#) = focal point		

The distribution of the algorithm and manual speeds were also compared to see if there was any significant difference between them. The manual speeds were the control group; therefore, the algorithm speeds were used for the observed frequency and the manually calculated speeds were used for the theoretical frequency. Table 4.6 summarizes the results from each test. All chi-squared tests were based on 99.5 percent confidence. Results show a significant difference for the sequences recorded 10 feet from the travel way and a height of 30 feet. Calculations for each sequence may be found in Appendix D.

Table 4.6: Summary of Chi-squared Comparison Test

Sequence	Significant Difference between Speeds?
D10H20(1)	No
D10H20(2)	No
D10H30(1)	Yes
D10H30(2)	Yes
D20H20(1)	No
D20H30(1)	No
NOTE: D = distance from travel way (ft), H = camera height (ft), (#) = focal point	

85^{th} Percentile Speed

A useful piece of information is the 85^{th} percentile speed. This is the speed used to determine the design speed for analyzing a roadway. Table 4.7 summarizes the 85^{th} percentile speeds calculated manually and by the algorithm for each of the sequences.

Table 4.7: Summary of 85^{th} percentile speed comparison

	Manual	Algorithm
D10 H20 (1)	76.70	75.00
D10 H20 (2)	80.74	77.00
D10 H30 (1)	75.76	92.95
D10 H30 (2)	70.53	89.00
D20 H20 (1)	74.83	73.00
D20 H30 (1)	73.05	73.00

NOTE: D = distance from travel way (ft), H = camera height (ft), (#) = focal point

As mentioned earlier, there is a significant discrepancy between the algorithm and manual speed for the sequences recorded 10 feet from the travel way and a height of 30 feet. There is not a significant difference for the other sequences.

CHAPTER FIVE

CONCLUSIONS

The research objectives were to assess the effects of the camera height and distance from the roadway on the accuracy of the algorithm. The author evaluated the system quantitatively on detection accuracy and qualitatively such as determining the cause of false detections. Results showed that the camera height and distance from the roadway had different effects on the accuracy of the collected volume, speed, and vehicle classification.

The camera height does have an effect on detection accuracy of the machine vision processor when the camera is placed close to the roadway. The difference in detection accuracy increased approximately three percent when the camera was raised from 20 to 30 feet. However, when the camera is located farther from the roadway, the height does not affect the accuracy. For the sequences recorded at 20 feet from the roadway, the difference in detection accuracy for the two heights was less than one percent. For the vehicles detected by the system, the accuracy of classification, for every sequence, was 97 percent or higher.

Previous studies have shown other virtual detection systems produce up to a 20 percent difference in estimating volume. Occlusions could not be blamed for the significant error since studies were conducted using traffic volumes consisting of five percent trucks or less. It has been concluded that the number of lanes has an effect on the amount of volume error. Shadows have proven to be an issue if it covers a significant portion of the detection zone. Studies show that this can cause the volume accuracy to fall below 90 percent. The new system produced a volume accuracy of 94 percent or higher for every video sequence. The traffic used to analysis the system included between 24 and 38 percent trucks.

Other virtual detection systems have issues with depth ambiguity, which has shown to cause a difference in detected vehicle speed of as much as 13 miles per hour. For the sequences recorded 10 feet from the travel way and a height of 30 feet, the system detected speeds, on average, 16 miles per hour higher than the actual speed. For all other sequences, the difference between the algorithm and manually calculated speeds was, at most, 2 miles per hour.

The system did have some problems occlusions, shadows, and double counting. Occlusions were more of an issue when the camera was located at lower heights. Shadows were an issue for one of the sequences. In this sequence, a vehicle shadow would cover the other lane causing a vehicle located in that shadow to be subtracted with the background. It cannot be concluded whether the amount of travel lane being covered by the shadow affects the accuracy since there was only one sequence that had shadows. Double counting may be contributed to coding errors and spillover. Sometimes the system would locate a large number of feature points and would assume that one vehicle was two or more.

CHAPTER SIX

RECOMMENDATIONS

There is still much research that can be done as a follow-up to this study. The first priority is to determine why there was such a significant difference in speeds for two of the sequences. The error was a systematic error for both sequences. The scenario which had detection errors was the ideal scenario; therefore, not many test sequences were used to calibrate this scenario. There were random errors with all of the sequences but those it would only be a difference in three or four miles per hour. Also, if this research is repeated, all sequences need to be recorded at the same time of day. This is the only way to get an accurate assessment of how lighting conditions impact the results.

The Federal Highway Administration recognizes 13 different vehicle classes. For simplistic purposes, this study only classified vehicles as either a passenger car or truck. More research can be done to include more specific vehicle classes. Not necessarily all 13 vehicle classes, but at least motorcycles, passenger cars, buses, and trucks.

Research needs to be done to include varying weather conditions, such as rain, foggy, and snow. Various intensities of rain, i.e. light and heavy rain, should be examined at to determine how much an impact the weather has on the vehicle detection accuracy of the system. The ability to test the system in snowy weather conditions is limited since the region in which this study was conducted does not get regular snowfall. Also, tests need to be done on roadways with three or more lanes, in each direction, to determine how the number of lanes affects the system's output. The purpose of more lanes would be to determine whether the addition of lanes would decrease the system's accuracy.

In addition to various weather conditions, research should look at heavier traffic volumes. As traffic volumes increase, speeds decrease and vehicle will be traveling closer together; this will create more occlusions. This way the system can be better assessed in determining how camera height and distance from the travel way affects volume accuracy.

APPENDICES

Appendix A

Comparison of Means and Variances

Sequence	D10H20(1)	D10H20(2)	D10H30(1)	D10H30(2)	D20H20(1)	D20H30(1)
α	0.05	0.05	0.05	0.05	0.05	0.05
μ_{1*}	70.532632	71.705208	69.078409	63.673	67.313592	66.058182
μ_{2**}	69.252632	70.9375	85.602273	79.7	66.76699	66.027273
n_{1*}	95	96	88	100	103	110
n_{2**}	95	96	88	100	103	110
s^2_{1*}	45.078179	59.211657	35.199414	34.623607	45.673539	45.707593
s^2_{2**}	38.807839	42.943421	49.437696	61.080808	33.788311	45.25613
c	0.5045785	0.502691	0.4465872	0.4441073	0.5020383	0.500117
df	187.98424	189.9945	172.03676	195.55634	203.99661	217.99999
t'	1.362	0.744	-16.849	-16.383	0.622	0.034
$t_{\alpha/2}$	1.980	1.980	1.980	1.980	1.980	1.980
Reject H_o?	No	No	Yes	Yes	No	No

Notes:

H_o: $\mu_1 - \mu_2 = 0$ * manual

H_a: $\mu_1 - \mu_2 \neq 0$ **algorithm

Figure A-1: Comparison of means for manually calculated and algorithm speeds.

Sequence	D10H20(1)	D10H20(2)	D10H30(1)	D10H30(2)	D20H20(1)	D20H30(1)
α	0.05	0.05	0.05	0.05	0.05	0.05
σ^2_{1*}	45.0781792	59.2116568	35.1994135	34.6236071	45.6735389	45.707593
σ^2_{2**}	38.8078387	42.9434211	49.4376959	61.0808081	33.7883114	45.2561301
n_{1*}	95	96	88	100	103	110
n_{2**}	95	96	88	100	103	110
F_{obs}	1.162	1.379	1.405	1.764	1.352	1.010
F	1.419	1.419	1.419	1.403	1.403	1.373
Reject H_o?	No	No	No	Yes	No	No

Notes:

H_o: $\sigma^2_1 = \sigma^2_2$ * manual

H_a: $\sigma^2_1 \neq \sigma^2_2$ **algorithm

Figure A-2: Comparison of variances for manually calculated and algorithm speeds.

Appendix B

Chi-Squared Analysis of Algorithm Speeds

Speed Group Upper Limit (mph)	Speed Group Lower Limit (mph)	Observed Frequency (n)	Upper Limit (Std. Normal) z_d	Probability $Z \le Z_d$	Prob. Of Occurrence in Group	Theoretical Frequency f	Combined Groups (n)	Combined Frequency f	X^2 Group
∞	90	1	∞	1.0000	0.0004	0.0384			
90	88	1	3.33	0.9996	0.0009	0.0864			
88	86	0	3.01	0.9987	0.0023	0.2208			
86	84	1	2.69	0.9964	0.0053	0.5088			
84	82	1	2.37	0.9911	0.0113	1.0848			
82	80	2	2.05	0.9798	0.0216	2.0736			
80	78	3	1.73	0.9582	0.0390	3.7440			
78	76	4	1.40	0.9192	0.0593	5.6928	13	13.4496	0.0150
76	74	7	1.08	0.8599	0.0835	8.0160	7	8.0160	0.1288
74	72	10	0.76	0.7764	0.1064	10.2144	10	10.2144	0.0045
72	70	14	0.44	0.6700	0.1222	11.7312	14	11.7312	0.4388
70	68	14	0.12	0.5478	0.1271	12.2016	14	12.2016	0.2651
68	66	14	-0.20	0.4207	0.1192	11.4432	14	11.4432	0.5713
66	64	8	-0.52	0.3015	0.1010	9.6960	8	9.6960	0.2967
64	62	6	-0.84	0.2005	0.0775	7.4400	6	7.4400	0.2787
62	60	5	-1.16	0.1230	0.0549	5.2704	5	5.2704	0.0139
60	58	3	-1.49	0.0681	0.0330	3.1680	5	6.5376	0.3616
58	56	2	-1.81	0.0351	0.0351	3.3696			
Total					**1.0000**	**96**	**96**	**96**	**2.3743**

df = 10 - 3 = 7	
0.9	2.833
0.95	2.167

p = prob (X2 >= 2.3743) 0.9344364

99.5% confident No Sig. Diff.

Figure B-1: Chi-squared results for sequence D = 10’, H = 20’ (video 1).

Speed Group									
Upper Limit (mph)	Lower Limit (mph)	Observed Frequency (n)	Upper Limit (Std. Normal) z_d	Probability $Z \le Z_d$	Prob. Of Occurrence in Group	Theoretical Frequency f	Combined Groups (n)	Combined Frequency f	X^2 Group
∞	90	4	∞	1.0000	0.0018	0.1764			
90	88	0	2.91	0.9982	0.0029	0.2842			
88	86	1	2.60	0.9953	0.0060	0.5880			
86	84	0	2.30	0.9893	0.0126	1.2348			
84	82	1	1.99	0.9767	0.0222	2.1756			
82	80	4	1.69	0.9545	0.0383	3.7534	10	8.2124	0.3891
80	78	5	1.38	0.9162	0.0563	5.5174	5	5.5174	0.0485
78	76	8	1.08	0.8599	0.0805	7.8890	8	7.8890	0.0016
76	74	6	0.77	0.7794	0.0986	9.6628	6	9.6628	1.3884
74	72	11	0.47	0.6808	0.1172	11.4856	11	11.4856	0.0205
72	70	12	0.16	0.5636	0.1193	11.6914	12	11.6914	0.0081
70	68	17	-0.14	0.4443	0.1179	11.5542	17	11.5542	2.5667
68	66	16	-0.45	0.3264	0.0998	9.7804	16	9.7804	3.9552
66	64	6	-0.75	0.2266	0.0820	8.0360	5	8.0360	1.1470
64	62	5	-1.06	0.1446	0.0577	5.6546	8	14.1708	2.6871
62	60	2	-1.36	0.0869	0.0394	3.8612			
60	58	1	-1.67	0.0475	0.0475	4.6550			
Total					**1.0000**	**98**	**98**	**98**	**12.2124**

df = 10 - 3 = 7	
0.05	14.07
0.1	12.02

p = prob (X2 >= 12.2124)	0.095308
99.5% confident	No Sig. Diff.

Figure B-2: Chi-squared results for sequence D = 10’, H = 20’ (video 2).

Speed Group									
Upper Limit (mph)	Lower Limit (mph)	Observed Frequency (n)	Upper Limit (Std. Normal) z_d	Probability $Z \leq Z_d$	Prob. Of Occurrence in Group	Theoretical Frequency f	Combined Groups (n)	Combined Frequency f	X^2 Group
∞	98	5	∞	1.0000	0.0392	3.4496			
98	96	2	1.76	0.9608	0.0302	2.6576	7	6.1072	0.1305
96	94	5	1.48	0.9306	0.0476	4.1888	5	4.1888	0.1571
94	92	5	1.19	0.8830	0.0644	5.6672	5	5.6672	0.0785
92	90	11	0.91	0.8186	0.0829	7.2952	11	7.2952	1.8814
90	88	9	0.63	0.7357	0.1026	9.0288	9	9.0288	0.0001
88	86	7	0.34	0.6331	0.1092	9.6096	7	9.6096	0.7087
86	84	10	0.06	0.5239	0.1149	10.1112	10	10.1112	0.0012
84	82	8	-0.23	0.4090	0.1040	9.1520	8	9.1520	0.1450
82	80	7	-0.51	0.3050	0.0931	8.1928	7	8.1928	0.1737
80	78	6	-0.80	0.2119	0.0718	6.3184	6	6.3184	0.0160
78	76	7	-1.08	0.1401	0.0548	4.8224	7	4.8224	0.9833
76	74	3	-1.37	0.0853	0.0358	3.1504	6	7.5064	0.3023
74	72	0	-1.65	0.0495	0.0227	1.9976			
72	70	2	-1.93	0.0268	0.0136	1.1968			
70	68	1	-2.22	0.0132	0.0132	1.1616			
Total					**1.0000**	**88**	**88**	**88**	**4.5779**

df = 12 - 3 = 9

0.75	5.899
0.9	4.168

p = prob (X2 >= 4.5779) 0.8644775

99.5% confident No Sig. Diff.

Figure B-3: Chi-squared results for sequence D = 10’, H = 30’ (video 1).

Speed Group										
Upper Limit (mph)	Lower Limit (mph)	Observed Frequency (n)	Upper Limit (Std. Normal) z_d	Probability $Z \leq Z_d$	Prob. Of Occurrence in Group	Theoretical Frequency f	Combined Groups (n)	Combined Frequency f	X^2 Group
∞	96	1	∞	1.0000	0.0183	1.8300			
96	94	3	2.09	0.9817	0.0153	1.5300			
94	92	6	1.83	0.9664	0.0246	2.4600	10	5.8200	3.0021
92	90	4	1.57	0.9418	0.0352	3.5200			
90	88	3	1.32	0.9066	0.0512	5.1200	7	8.6400	0.3113
88	86	6	1.06	0.8554	0.0644	6.4400	6	6.4400	0.0301
86	84	7	0.81	0.7910	0.0822	8.2200	7	8.2200	0.1811
84	82	9	0.55	0.7088	0.0947	9.4700	9	9.4700	0.0233
82	80	11	0.29	0.6141	0.0981	9.8100	11	9.8100	0.1444
80	78	7	0.04	0.5160	0.1031	10.3100	7	10.3100	1.0627
78	76	10	-0.22	0.4129	0.0937	9.3700	10	9.3700	0.0424
76	74	9	-0.47	0.3192	0.0865	8.6500	9	8.6500	0.0142
74	72	7	-0.73	0.2327	0.0716	7.1600	7	7.1600	0.0036
72	70	9	-0.99	0.1611	0.0536	5.3600	9	5.3600	2.4719
70	68	4	-1.24	0.1075	0.0407	4.0700	8	10.7500	0.7035
68	66	1	-1.50	0.0668	0.0267	2.6700			
66	64	2	-1.75	0.0401	0.0179	1.7900			
64	62	1	-2.01	0.0222	0.0222	2.2200			
Total					**0.9599**	**100**	**100**	**100**	**7.9904**

df = 11 - 3 = 8

0.25	10.22
0.5	7.344

p = prob (X2 >= 7.9904) 0.4438082

99.5% confident No Sig. Diff.

Figure B-4: Chi-squared results for sequence D = 10’, H = 30’ (video 2).

Speed Group									
Upper Limit (mph)	Lower Limit (mph)	Observed Frequency (n)	Upper Limit (Std. Normal) z_d	Probability $Z \leq Z_d$	Prob. Of Occurrence in Group	Theoretical Frequency f	Combined Groups (n)	Combined Frequency f	X^2 Group
∞	80	1	∞	1.0000	0.0113	1.1639			
80	78	1	2.28	0.9887	0.0155	1.5965			
78	76	5	1.93	0.9732	0.0291	2.9973	7	5.7577	0.2680
76	74	6	1.59	0.9441	0.0516	5.3148	6	5.3148	0.0883
74	72	12	1.24	0.8925	0.0766	7.8898	12	7.8898	2.1412
72	70	11	0.90	0.8159	0.1036	10.6708	11	10.6708	0.0102
70	68	14	0.56	0.7123	0.1291	13.2973	14	13.2973	0.0371
68	66	9	0.21	0.5832	0.1349	13.8947	9	13.8947	1.7243
66	64	10	-0.13	0.4483	0.1327	13.6681	10	13.6681	0.9844
64	62	10	-0.48	0.3156	0.1095	11.2785	10	11.2785	0.1449
62	60	14	-0.82	0.2061	0.0831	8.5593	14	8.5593	3.4584
60	58	5	-1.16	0.1230	0.0575	5.9225	5	5.9225	0.1437
58	56	4	-1.51	0.0655	0.0333	3.4299	5	6.7465	0.4521
56	54	1	-1.85	0.0322	0.0322	3.3166			
Total					**1.0000**	**103**	**103**	**103**	**9.4527**

df = 11 - 3 = 8	
0.25	10.22
0.5	7.344

p = prob (X2 >= 9.4527) 0.3167018

99.5% confident No Sig. Diff.

Figure B-5: Chi-squared results for sequence D = 20’, H = 20’.

Speed Group									
Upper Limit (mph)	Lower Limit (mph)	Observed Frequency (n)	Upper Limit (Std. Normal) z_d	Probability $Z \leq Z_d$	Prob. Of Occurrence in Group	Theoretical Frequency f	Combined Groups (n)	Combined Frequency f	X^2 Group
∞	80	2	∞	1.0000	0.0188	2.0680			
80	78	3	2.08	0.9812	0.0187	2.0570			
78	76	9	1.78	0.9625	0.0319	3.5090			
76	74	1	1.48	0.9306	0.0476	5.2360	15	12.8700	0.3525
74	72	8	1.19	0.8830	0.0697	7.6670	8	7.6670	0.0145
72	70	12	0.89	0.8133	0.0909	9.9990	12	9.9990	0.4004
70	68	11	0.59	0.7224	0.1083	11.9130	11	11.9130	0.0700
68	66	12	0.29	0.6141	0.1141	12.5510	12	12.5510	0.0242
66	64	12	0.00	0.5000	0.1179	12.9690	12	12.9690	0.0724
64	62	11	-0.30	0.3821	0.1078	11.8580	11	11.8580	0.0621
62	60	8	-0.60	0.2743	0.0902	9.9220	8	9.9220	0.3723
60	58	9	-0.90	0.1841	0.0671	7.3810	9	7.3810	0.3551
58	56	7	-1.19	0.1170	0.0489	5.3790	7	5.3790	0.4885
56	54	2	-1.49	0.0681	0.0314	3.4540	5	7.4910	0.8283
54	52	2	-1.79	0.0367	0.0184	2.0240			
52	50	1	-2.09	0.0183	0.0183	2.0130			
Total					**1.0000**	**110**	**110**	**110**	**3.0403**

df = 11 - 3 = 8	
0.9	3.199
0.95	2.733

p = prob (X2 >= 7.2523)	0.9170239
99.5% confident	No Sig. Diff.

Figure B-6: Chi-squared results for sequence D = 20’, H = 30’.

Appendix C

Chi-Squared Analysis of Manual Speeds

Speed Group		Observed Frequency (n)	Upper Limit (Std. Normal) z_d	Probability $Z \leq Z_d$	Prob. Of Occurrence in Group	Theoretical Frequency f	Combined Groups (n)	Combined Frequency f	X^2 Group
Upper Limit (mph)	Lower Limit (mph)								
∞	90	1	∞	1.0000	0.0019	0.1900			
90	88	0	2.90	0.9981	0.0028	0.2800			
88	86	0	2.60	0.9953	0.0060	0.6000			
86	84	2	2.30	0.9893	0.0115	1.1500			
84	82	1	2.01	0.9778	0.0214	2.1400			
82	80	3	1.71	0.9564	0.0357	3.5700			
80	78	6	1.41	0.9207	0.0542	5.4200			
78	76	3	1.11	0.8665	0.0755	7.5500	16	20.9000	1.1488
76	74	10	0.81	0.7910	0.0925	9.2500	10	9.2500	0.0608
74	72	9	0.52	0.6985	0.1114	11.1400	9	11.1400	0.4111
72	70	12	0.22	0.5871	0.1190	11.9000	12	11.9000	0.0008
70	68	20	-0.08	0.4681	0.1161	11.6100	20	11.6100	6.0631
68	66	8	-0.38	0.3520	0.1037	10.3700	8	10.3700	0.5416
66	64	8	-0.68	0.2483	0.0823	8.2300	8	8.2300	0.0064
64	62	4	-0.97	0.1660	0.0640	6.4000	17	16.6000	0.0096
62	60	8	-1.27	0.1020	0.0438	4.3800			
60	58	3	-1.57	0.0582	0.0275	2.7500			
58	56	2	-1.87	0.0307	0.0307	3.0700			
Total					**1.0000**	**100**	**100**	**100**	**8.2423**

df = 8 - 3 = 5	
0.1	9.236
0.25	6.626

p = prob (X2 >= 8.2423)	0.1571079
99.5% confident	No Sig. Diff.

Figure C-1: Chi-squared results for sequence D = 10’, H = 20’ (video 1).

Speed Group									
Upper Limit (mph)	Lower Limit (mph)	Observed Frequency (n)	Upper Limit (Std. Normal) z_d	Probability $Z \le Z_d$	Prob. Of Occurrence in Group	Theoretical Frequency f	Combined Groups (n)	Combined Frequency f	X^2 Group
∞	90	1	∞	1.0000	0.0087	0.9570			
90	88	0	2.38	0.9913	0.0083	0.9130			
88	86	4	2.12	0.9830	0.0144	1.5840			
86	84	2	1.86	0.9686	0.0234	2.5740			
84	82	2	1.60	0.9452	0.0353	3.8830			
82	80	6	1.34	0.9099	0.0500	5.5000	15	15.4110	0.0110
80	78	3	1.08	0.8599	0.0660	7.2600	5	7.2600	0.7035
78	76	7	0.82	0.7939	0.0816	8.9760	8	8.9760	0.1061
76	74	6	0.56	0.7123	0.0944	10.3840	6	10.3840	1.8509
74	72	7	0.30	0.6179	0.1019	11.2090	11	11.2090	0.0039
72	70	9	0.04	0.5160	0.1031	11.3410	12	11.3410	0.0383
70	68	18	-0.22	0.4129	0.0973	10.7030	17	10.7030	3.7048
68	66	9	-0.48	0.3156	0.0860	9.4600	16	9.4600	4.5213
66	64	9	-0.74	0.2296	0.0709	7.7990	5	7.7990	1.0045
64	62	8	-1.00	0.1587	0.0549	6.0390	8	6.0390	0.6368
62	60	5	-1.26	0.1038	0.0395	4.3450	7	15.5430	4.6955
60	58	1	-1.52	0.0643	0.0643	7.0730			
58	56	1	-1.78	0.0375	0.0375	4.1250			
Total					**1.0000**	**110**	**110**	**114**	**17.2766**

df = 11 - 3 = 8

0.025	17.63
0.05	15.51

p = prob (X2 >= 17.2766) 0.0291672

99.5% confident No Sig. Diff.

Figure C-2: Chi-squared results for sequence D = 10’, H = 20’ (video 2).

Speed Group									
Upper Limit (mph)	Lower Limit (mph)	Observed Frequency (n)	Upper Limit (Std. Normal) z_d	Probability $Z \leq Z_d$	Prob. Of Occurrence in Group	Theoretical Frequency f	Combined Groups (n)	Combined Frequency f	X^2 Group
∞	85	3	∞	1.0000	0.0037	0.3774			
85	83	0	2.68	0.9963	0.0057	0.5814			
83	81	8	2.35	0.9906	0.0128	1.3056			
81	79	0	2.01	0.9778	0.0253	2.5806			
79	77	11	1.67	0.9525	0.0426	4.3452	22	9.1902	17.8550
77	75	10	1.34	0.9099	0.0686	6.9972	10	6.9972	1.2886
75	73	13	1.00	0.8413	0.0959	9.7818	13	9.7818	1.0588
73	71	0	0.66	0.7454	0.1199	12.2298			
71	69	14	0.32	0.6255	0.1295	13.2090	14	25.4388	5.1436
69	67	10	-0.01	0.4960	0.1328	13.5456	10	13.5456	0.9281
67	65	12	-0.35	0.3632	0.1181	12.0462	12	12.0462	0.0002
65	63	4	-0.69	0.2451	0.0912	9.3024	12	16.1364	1.0603
63	61	8	-1.02	0.1539	0.0670	6.8340			
61	59	5	-1.36	0.0869	0.0423	4.3146	9	8.8638	0.0021
59	57	2	-1.70	0.0446	0.0239	2.4378			
57	55	2	-2.04	0.0207	0.0207	2.1114			
Total					**1.0000**	**102**	**102**	**102**	**27.3366**

df = 8 - 3 = 5

0.001	20.52
0.005	16.75

p = prob (X2 >= 27.3366) -0.006233

99.5% confident Sig. Diff.

Figure C-3: Chi-squared results for sequence D = 10', H = 30' (video 1).

Speed Group									
Upper Limit (mph)	Lower Limit (mph)	Observed Frequency (n)	Upper Limit (Std. Normal) z_d	Probability $Z \leq Z_d$	Prob. Of Occurrence in Group	Theoretical Frequency f	Combined Groups (n)	Combined Frequency f	X^2 Group
∞	76	0	∞	1.0000	0.0183	1.8849			
76	74	3	2.09	0.9817	0.0209	2.1527			
74	72	9	1.76	0.9608	0.0386	3.9758	12	8.0134	1.9833
72	70	9	1.42	0.9222	0.0623	6.4169	9	6.4169	1.0398
70	68	9	1.08	0.8599	0.0895	9.2185	9	9.2185	0.0052
68	66	11	0.74	0.7704	0.1150	11.8450	11	11.8450	0.0603
66	64	0	0.40	0.6554	0.1315	13.5445			
64	62	30	0.06	0.5239	0.1342	13.8226	30	27.3671	0.2533
62	60	7	-0.28	0.3897	0.1221	12.5763	7	12.5763	2.4725
60	58	8	-0.62	0.2676	0.0991	10.2073	8	10.2073	0.4773
58	56	7	-0.96	0.1685	0.0717	7.3851	7	7.3851	0.0201
56	54	5	-1.30	0.0968	0.0463	4.7689	5	4.7689	0.0112
54	52	4	-1.64	0.0505	0.0266	2.7398	5	5.2015	0.0078
52	50	0	-1.98	0.0239	0.0137	1.4111			
50	48	1	-2.32	0.0102	0.0102	1.0506			
Total					**1.0000**	**103**	**103**	**103**	**6.3308**

df = 10 - 3 = 7

0.5	6.346
0.75	4.255

p = prob (X2 >= 6.3308) 0.5018165

99.5% confident No Sig. Diff.

Figure C-4: Chi-squared results for sequence D = 10', H = 30' (video 2).

Speed Group										
Upper Limit (mph)	Lower Limit (mph)	Observed Frequency (n)	Upper Limit (Std. Normal) z_d	Probability $Z \leq Z_d$	Prob. Of Occurrence in Group	Theoretical Frequency f	Combined Groups (n)	Combined Frequency f	X^2 Group
∞	80	7	∞	1.0000	0.0301	3.3712			
80	78	4	1.88	0.9699	0.0270	3.0240			
78	76	3	1.58	0.9429	0.0414	4.6368	14	11.0320	0.7985
76	74	8	1.29	0.9015	0.0626	7.0112	8	7.0112	0.1395
74	72	6	0.99	0.8389	0.0840	9.4080	6	9.4080	1.2345
72	70	7	0.69	0.7549	0.0995	11.1440	7	11.1440	1.5410
70	68	15	0.40	0.6554	0.1156	12.9472	15	12.9472	0.3255
68	66	15	0.10	0.5398	0.1151	12.8912	15	12.8912	0.3450
66	64	4	-0.19	0.4247	0.1126	12.6112			
64	62	12	-0.49	0.3121	0.0973	10.8976	16	23.5088	2.3983
62	60	19	-0.79	0.2148	0.0747	8.3664			
60	58	2	-1.08	0.1401	0.0563	6.3056	21	14.6720	2.7293
58	56	4	-1.38	0.0838	0.0363	4.0656	10	9.3856	0.0402
56	54	6	-1.67	0.0475	0.0475	5.3200			
Total					**1.0000**	**112**	**112**	**112**	**9.5517**

df = 9 - 3 = 6	
0.1	10.64
0.25	7.841

p = prob (X2 >= 9.5517)	0.1583217
99.5% confident	No Sig. Diff.

Figure C-5: Chi-squared results for sequence D = 20’, H = 20’ (video 1).

Speed Group										
Upper Limit (mph)	Lower Limit (mph)	Observed Frequency (n)	Upper Limit (Std. Normal) z_d	Probability $Z \leq Z_d$	Prob. Of Occurrence in Group	Theoretical Frequency f	Combined Groups (n)	Combined Frequency f	X^2 Group
∞	80	1	∞	1.0000	0.0188	2.1056			
80	78	6	2.06	0.9812	0.0187	2.0944			
78	76	0	1.77	0.9625	0.0319	3.5728	7	7.7728	0.0768
76	74	8	1.47	0.9306	0.0476	5.3312	8	5.3312	1.3360
74	72	6	1.17	0.8830	0.0697	7.8064	6	7.8064	0.4180
72	70	15	0.88	0.8133	0.0909	10.1808	15	10.1808	2.2812
70	68	11	0.58	0.7224	0.1083	12.1296	11	12.1296	0.1052
68	66	13	0.29	0.6141	0.1141	12.7792	13	12.7792	0.0038
66	64	0	-0.01	0.5000	0.1179	13.2048			
64	62	23	-0.30	0.3821	0.1078	12.0736	23	25.2784	0.2054
62	60	10	-0.60	0.2743	0.0902	10.1024	10	10.1024	0.0010
60	58	6	-0.90	0.1841	0.0671	7.5152	6	7.5152	0.3055
58	56	6	-1.19	0.1170	0.0489	5.4768	6	5.4768	0.0500
56	54	3	-1.49	0.0681	0.0314	3.5168	7	7.6272	0.0516
54	52	3	-1.78	0.0367	0.0184	2.0608			
52	50	1	-2.08	0.0183	0.0183	2.0496			
Total					**1.0000**	**112**	**112**	**112**	**4.8345**

df = 11 - 3 = 8	
0.75	5.071
0.9	3.199

p = prob (X2 >=4.8345) 0.7689489

99.5% confident No Sig. Diff.

Figure C-6: Chi-squared results for sequence D = 20’, H = 30’ (video 1).

Appendix D

Chi-Squared Comparison of Manual and Algorithm Speeds

Speeds (mph)	Observed Frequency n	Theoretical Frequency F	χ2
58-60	5	4	0.2500
61-63	11	9	0.4444
64-66	13	17	0.9412
67-69	23	20	0.4500
70-72	18	11	4.4545
73-75	13	18	1.3889
76-78	6	8	0.5000
79-∞	6	8	0.5000
Total	**95**	**95**	**8.9291**

df = 7

0.25	9.037
0.5	6.346

$P(X^2>=8.9261)$	0.26002831
99.5 % Confidence	Not Sig. Diff.

Figure D-1: Comparison for sequence D = 10’, H = 20’ (video 1).

Speeds (mph)	Observed Frequency n	Theoretical Frequency F	χ2
61-63	8	10	0.4000
64-66	16	22	1.6364
67-69	23	18	1.3889
70-72	19	9	11.1111
73-75	10	13	0.6923
76-78	10	9	0.1111
79-81	6	6	0.0000
82-∞	5	10	2.5000
Total	**97**	**97**	**17.8398**

df = 7

0.01	18.48
0.025	16.01

$P(X^2>=17.8398)$	0.01388796
99.5 % Confidence	Not Sig. Diff.

Figure D-2: Comparison for sequence D = 10’, H = 20’ (video 2).

Speeds (mph)	Observed Frequency n	Theoretical Frequency F	χ2
58-60	0	9	9.0000
61-63	0	8	8.0000
64-66	0	16	16.0000
67-69	0	10	10.0000
70-72	0	14	14.0000
73-75	6	23	12.5652
76-78	11	8	1.1250
79-81	9	0	0.0000
82-84	10	0	0.0000
85-87	15	0	0.0000
88-90	14	0	0.0000
91-93	11	0	0.0000
94-96	6	0	0.0000
97-99	6	0	0.0000
Total	**88**	**88**	**70.6902**

df = 13

0.001	34.53
0.005	29.82

$P(X^2 >= 70.6902)$	-0.02970931
99.5 % Confidence	Sig. Diff.

Figure D-3: Comparison for sequence D = 10’, H = 30’ (video 1).

Speeds (mph)	Observed Frequency n	Theoretical Frequency F	χ2
52-54	0	5	5.0000
55-57	0	12	12.0000
58-60	0	15	15.0000
61-63	0	13	13.0000
64-66	0	27	27.0000
67-69	8	9	0.1111
70-72	12	8	2.0000
73-75	13	11	0.3636
76-78	14	0	0.0000
79-81	14	0	0.0000
82-84	12	0	0.0000
85-87	10	0	0.0000
88-∞	17	0	0.0000
Total	**100**	**100**	**69.4747**

df = 12

0.001	32.91
0.005	28.3

$P(X^2 >= 69.4747)$	-0.03072646
99.5 % Confidence	Sig. Diff.

Figure D-4: Comparison for sequence D = 10’, H = 30’ (video 2).

Speeds (mph)	Observed Frequency n	Theoretical Frequency F	χ2		
				df = 7	
55-57	5	5	0.0000		
58-60	12	14	0.2857		
61-63	17	14	0.6429		
64-66	17	11	3.2727	0.25	9.037
67-69	16	18	0.2222	0.5	6.346
70-72	18	15	0.6000		
73-75	11	14	0.6429	$P(X^2>=7.7497)$	0.36959203
76-∞	7	12	2.0833		
				99.5 % Confidence	Not Sig. Diff.
Total	**103**	**103**	**7.7497**		

Figure D-5: Comparison for sequence D = 20’, H = 20’ (video 1).

Speeds (mph)	Observed Frequency n	Theoretical Frequency F	χ2		
				df = 6	
55-57	12	12	0.0000		
58-60	14	16	0.2500		
61-63	14	10	1.6000	0.25	7.841
64-66	19	25	1.4400	0.5	5.348
67-69	16	11	2.2727		
70-72	17	15	0.2667		
73-∞	18	21	0.4286	$P(X^2>=6.2580)$	0.40874796
				99.5 % Confidence	Not Sig. Diff.
Total	**110**	**110**	**6.2580**		

Figure D-6: Comparison for sequence D = 20’, H = 30’ (video 1).

REFERENCES

Barber, A., et. al. "Traffic Sensor Using a Color Vision Method," *Proceedings of the International Society for Optical Engineering*, Vol. 2902 (1997): 156-164.

Bebis, George, Ronald Miller, and Zehang Sun. “Quantized Wavelet Features and Support Vector Machines for On-Road Vehicle Detection.” *Proceedings of the 7th International Conference on Control, Automation, Robotics and Vision* (2002): 1641-1646

Betke, Margrit, Esin Haritaoglu, Larry S. Davis. “Multiple Vehicle Detection and Tracking.” *The International Society for Optical Engineering*. Vol. 2962 (1997): 104-110.

Betke, Margrit, Esin Haritaoglu, Larry S. Davis. “Real-time Multiple Vehicle Detection and Tracking from a Moving Vehicle.” *Machine Vision and Applications*. Vol. 12, No. 2 (2000): 69-83.

Beymer, D. “A Real Time Computer Vision System for Measuring Traffic Parameters.” *IEEE Conference on Computer Vision and Pattern Recognition* (1997): 495–501.

Birchfield, Stanley T., et. al. “Automated Traffic Surveillance Using Low-Angle Cameras.” Final Project Report. (2006)

Carlson, Brian. “Clearing the Congestion: Vision Makes Traffic Control Intelligent.” *Advanced Imaging*. Vol. 12 No. 2 (1997): 54-57.

Cathy, F.W., D. Daily, and S. Pumrin. “An Algorithm to Estimate Mean Traffic Speed Using Uncalibrated Cameras.” *IEEE Conference for Intelligent Transportation Systems* (2000): 98–107.

Charkari, N. Moghadam, and Hideo Mori, “New Approach for Real Time Moving Vehicle Detection.” *1993 International Conference on Intelligent Robots and Systems*. (1993): 273-278.

Cheung, S. C. and Chandrika Kamath. “Robust Techniques for Background Subtraction in Urban Traffic Video.” *Proceedings of the SPIE – The International Society for Optical Engineering*. Vol. 5308 No. 1 (2004): 881-92.

Cucchiara, Rita, et. al. “Detecting Moving Shadows: Algorithms and evaluation.” *IEEE Transactions on Pattern Analysis and Machine Intelligence*, Vol. 25 No. 7 (2003): 918-923.

Dandilis, K., D. Koller, and H. H. Nagel. "Model Based Object Tracking in Monocular Image Sequences of Road Traffic Scenes." *International Journal of Computer Vision*, Vol. 10, No. 3 (1993): 257–281.

Econolite Corporation. "Autoscope." Econolite Corporate Site. 6 December 2007. Accessed: 6 December 2007. http://www.econolite.com/products/autoscope/default.asp

Ferryman, J.M., S. J. Maybank, A. D. Worral. "Learning Enhanced 3D Models for Vehicle Tracking." *British Machine Vision Conference* (1998): 873–882.

Gloyer, Brian, et al. "Video-Based Freeway Monitoring System Using Recursive Vehicle Tracking." *The International Society of Optical Engineering*. Vol. 2421 (1995): 173-180.

Grenard, Jeromy L., D. Bullock, and A. Tarko. "Evaluation of Selected Video Detection Systems at Signalized Intersections." Publication FHWA/IN/JTRP-2001/22, Joint Transportation Research Program, Indiana Department of Transportation, Purdue University (2001).

Gupte, S., et. al.. "Detection and Classification of Vehicles." *IEEE Transactions on Intelligent Transportation Systems*, Vol.3, No.1 (2002): 37–47.

Haag, M. and H. Nagel. "Combination of Edge Element and Optical Flow Estimate for 3D-Model-Based Vehicle Tracking in Traffic Image Sequences." *International Journal of Computer Vision*, Vol. 35, No. 3 (1999): 295–319.

Hinz, S., J. Reitberger, and C. Schlosser. "Automatic Car Detection in High Resolution Urban Scenes Based on an Adaptive 3D-Model." *EEE/ISPRS Joint Workshop on Remote Sensing and Data Fusion over Urban Areas, Berlin* (2003): 98–107.

Kamijo, Shunsuke, et. al. "Development and Evaluation of Real-time Video Surveillance System on Highway Based on Semantic Hierarchy and Decision Surface." *2005 International Conference on Systems, Man and Cybernetics*. (2005): 840-846.

Kanhere, Neeraj K., Stanley T. Birchfield, Wayne A. Sarasua. "Automatic Camera Calibration Using Pattern Detection for Vision-Based Speed Sensing." *2008 Transportation Research Board Annual Meeting*. Transportation Research Board (2007).

Koller, D., J. Weber, and J. Malik. "Robust Multiple Car Tracking with Occlusion Reasoning." *European Conference on Computer Vision* (1994): 189–196.

Kumar, P., et al. "Framework for Real-Time Behavior Interpretation from Traffic Video." *IEEE Transactions on Intelligent Transportation Systems*. Vol. 6 No. 1 (2005): 43-53.

Lu, Yean-Jye, Yuen-Hung Hsu, Guan C. Tan. "Application of the Image Analysis Technique to Detect Left-Turning Vehicles at Intersections." *Transportation Research Record*. No. 1194 (1988): 120-128.

Magee, D. "Tracking Multiple Vehicles Using Foreground, Background and Motion Models." *Proceedings of ECCV Workshop on Statistical Methods in Video Processing* (2002).

Mak, Chin Long, and Henry S.L. Fan. "Heavy Flow-Based Incident Detection Algorithm Using Information from Two Adjacent Detector Stations." *Journal of Intelligent Transportation Systems*. Vol. 10 No. 1 (2006): 23-31.

Michalopoulos, Panos G., "Vehicle Detection Video through Image Processing: The Autoscope System." *IEEE Transactions on Vehicular Technology*. Vol. 40 No. 1 (1991): 21-29.

Michalopoulos, Panos G., Craig Anderson, and Richard Jacobson. "Cost Benefit Analysis of Video-Based Vehicle Detection." *Proceedings of the International Conference on Applications of Advanced Technologies in Transportation Engineering*. 4th International Conference on Applications of Advanced Technologies in Transportation Engineering (1996): 176-182.

Oh, J., and J.D. Leonard. "Vehicle Detection Using Video Image Processing System: Evaluation of PEEK VideoTrak." *Journal of Transportation Engineering*. Vol. 129 No. 4 (2003): 462-465.

Ott, R. Lyman and Michael Longnecker. *Introduction to Statistical Methods and Data Analysis: 5th Edition*. Pacific Grove, CA: Thomson Learning, Inc., 2001. pp. 275-276, 358, 1113.

P. Rosin and T. Ellis. "Image Difference Threshold Strategies and Shadow Detection." *Proceedings of the 6th British Machine Vision Conference*. Vol. 1 (1995): 347-356.

PEEK Traffic Corporation. "VideoTrak." Quixote Traffic Corporate Site. 27 February 2007. Accessed: 14 August 2007. http://www.peektrafficinc.com/products/video/videotrak.html

Prati, Andrea, et. al. "Detecting Moving Shadows: Algorithms and Evaluation." *IEEE Transactions on Pattern Analysis and Machine Intelligence.* Vol. 25 No. 7 (2003): 918-923.

Qiu, Zhijun, and Danya Yao. "Kalman Filtering Used in Video-Based Traffic Monitoring System." *Journal of Intelligent Transportation Systems*. Vol. 10 No. 1 (2006): 15-21.

Rabie, Tamer, Baher Abdulhai, and Amer Shalaby. "Mobile Active-Vision Traffic Surveillance System for Urban Networks." *Computer-Aided Civil and Infrastructure Engineering*. Vol. 20 No. 4 (2005): 231-241.

Rajagopalan, A.N. and R. Chellappa, "Vehicle Detection and Tracking in Video." *IEEE International Conference on Image Processing*. Vol. 1 (2000): 351-354.

Rhodes, Avery, Edward J. Smaglik, Darcy Bullock. "Vendor Comparison of Video Detection Systems." Publication FHWA/IN/JTRP-2005/30, Joint Transportation Research Program, Indiana Department of Transportation, Purdue University (2005).

Rhodes, Avery, et al. "Evaluation of the Accuracy of Stop Bar Video Vehicle Detection at Signalized Intersections." *Transportation Research Record*. No. 1925 (2005): 134-145.

Rhodes, Avery, Kristofer Jennings, Darcy Bullock. "Impact of Camera and Lighting Position on Video Detection Precision." Publication FHWA/IN/JTRP-2005/29, Joint Transportation Research Program, Indiana Department of Transportation, Purdue University (2005).

Roess, Roger P., Elena S. Prassas, and William R. McShane. *Traffic Engineering: Third Edition*. Lebanon, IN: Prentice Hall, 2004. pp. 153-155, 219-221.

Saunier, N. and T. Sayed. "A Feature-Based Tracking Algorithm for Vehicles in Intersections." *Third Canadian Conference on Computer and Robot Vision* (2006).

Sun, Z., G. Bebis, and R. Miller. "On-Road Vehicle Detection Using Evolutionary Gabor Filter Optimization." *IEEE Transactions on Intelligent Transportation Systems*. Vol. 6 No. 2 (2005): 125-137.